

Mechanotransduction of mitochondrial AMPK and its distinct role in flow-induced breast cancer cell migration

Hannah E. Steele¹, Yunxia Guo^{1,2}, Bai-Yan Li², Sungsoo Na^{1*}

¹Department of Biomedical Engineering, Indiana University-Purdue University Indianapolis, Indianapolis, IN 46202, USA

²Department of Pharmacology, School of Pharmacy, Harbin Medical University, Harbin 150081, China

* Corresponding author

Sungsoo Na, PhD

Department of Biomedical Engineering

Indiana University-Purdue University Indianapolis

723 West Michigan Street, SL220, Indianapolis, IN 46202, USA

Phone: 1-317-278-2384

Fax: 1-317-278-2455

E-mail: sungna@iu.edu

This is the author's manuscript of the article published in final edited form as:

Steele, H. E., Guo, Y., Li, B.-Y., & Na, S. (2019). Mechanotransduction of mitochondrial AMPK and its distinct role in flow-induced breast cancer cell migration. *Biochemical and Biophysical Research Communications*, 514(2), 524–529. <https://doi.org/10.1016/j.bbrc.2019.04.191>

Abstract

The biophysical microenvironment of the tumor site has significant impact on breast cancer progression and metastasis. The importance of altered mechanotransduction in cancerous tissue has been documented, yet its role in the regulation of cellular metabolism and the potential link between cellular energy and cell migration remain poorly understood. In this study, we investigated the role of mechanotransduction in AMP-activated protein kinase (AMPK) activation in breast cancer cells in response to interstitial fluid flow (IFF). Additionally, we explored the involvement of AMPK in breast cancer cell migration. IFF was applied to the 3D cell-matrix construct. The subcellular signaling activity of Src, FAK, and AMPK was visualized in real-time using fluorescent resonance energy transfer (FRET). We observed that breast cancer cells (MDA-MB-231) are more sensitive to IFF than normal epithelial cells (MCF-10A). AMPK was activated at the mitochondria of MDA-MB-231 cells by IFF, but not in other subcellular compartments (i.e., cytosol, plasma membrane, and nucleus). The inhibition of FAK or Src abolished flow-induced AMPK activation in the mitochondria of MDA-MB-231 cells. We also observed that global AMPK activation reduced MDA-MB-231 cell migration. Interestingly, specific AMPK inhibition in the mitochondria reduced cell migration and blocked flow-induced cell migration. Our results suggest the linkage of FAK/Src and mitochondria-specific AMPK in mechanotransduction and the differential role of AMPK in breast cancer cell migration depending on its subcellular compartment-specific activation.

Keywords

mechanotransduction, metabolic signaling, AMPK, Src, FAK

1. Introduction

The altered biophysical microenvironment of the tumor plays significant roles in cancer progression and metastasis. Malignant epithelial mammary cells form primary tumors out of mammary ducts and into the surrounding extracellular matrix (ECM). This process places unwanted pressure on its confined ECM and increases IFF, which in turn promotes cancer cell migration and invasion [1-3]. This IFF-induced cell migration is mediated by integrin-mediated mechanotransduction [3-8]. For example, flow-induced shear stress exerted on breast cancer cells results in β 1-integrin activation [3, 6-9]. Signals initiated at these focal adhesions are then transduced into cells via activation of integrin-associated tyrosine kinases – namely, Src and FAK [7, 8, 10, 11]. They are both highly expressed in metastatic breast cancer cells and their inhibition has been reported to suppress cancer cell migration [6, 7, 10, 12, 13].

AMPK is a serine/threonine protein kinase that regulates cellular energy homeostasis [14-17]. It senses the ratios of AMP /ATP and ADP/ATP. As the ratios increase, the amount of viable energy inside the cell drops and AMPK is activated. AMPK has been mainly considered a metabolic tumor suppressor. AMPK activity is diminished in breast cancer, and its activation in metastatic cancer cells inhibits cell growth and migration [14, 18]. The efficacy of clinical AMPK activators in preventing tumor progression and metastasis is attributed in part to the inhibition of cell migration [18]. In spite of AMPK downregulation in tumor cells, AMPK has garnered much attention for having dual functions in cancer. Several lines of evidence show that when AMPK is “on” it stimulates mitophagy and enhances the metabolic survival of cancer cells; however, AMPK activation also inhibits tumor growth and proliferation [16, 17]. When AMPK is “off” it enables unchecked cancer growth and proliferation, but the metabolic plasticity

of cells is diminished [16, 17]. This paradoxical nature of AMPK in cancer has led to the hypothesis that different subcellular activation of AMPK might determine the AMPK's final role in cancer [15, 17]. Indeed, there have been efforts to identify the role of compartmentalized AMPK signaling in response to pharmacological AMPK modulators [19-21]. While accumulating evidence shows that the biophysical microenvironment plays a crucial role in cancer cell metabolism [22], it is unclear whether the subcellular compartment-specific AMPK responds to the upstream biophysical cues and determines discrete downstream cellular processes that can have pro- or anti-tumorigenic roles in cancer.

In this study, we employed genetically encoded biosensors to visualize Src and FAK as well as AMPK activities at the specific subcellular locations in response to IFF in the 3D collagen-Matrigel matrices. The AMPK responses of MDA-MB-231 cells were compared with those of MCF-10A cells. We investigated the role of global AMPK as well as mitochondria-specific AMPK on flow-induced cell migration. The role of Src and FAK on mitochondria-specific AMPK activities under flow was also examined.

2. Materials and Methods

2.1 Biosensors and plasmids

The FRET-based biosensors were used to observe subcellular activities of Src, FAK, and AMPK. The development and specificity of these biosensors were previously described [23-25]. The Src biosensor (Lyn-Src) consists of a cyan fluorescent protein (CFP), the SH2 domain from c-Src, a yellow fluorescent protein (YFP), and Src substrate peptide [23]. Similarly, the FAK biosensor (Lyn-FAK) is comprised of a CFP, SH2 domain, YFP, and FAK substrate peptide [24]. The

AMPK biosensors consist of a CFP, an FHA1 binding domain, an AMPK substrate peptide, and a YFP variant (cpVE172) [25]. The subcellular compartment-specific AMPK biosensors employed here were Cyto-, PM-, Nuc-, and Mito-AMPK, specific to the cytosol, plasma membrane, nucleus, and mitochondria, respectively. An AMPK inhibitor peptide targeted to the mitochondria (mito-AIP) was used. The development and accuracy of mito-AIP was previously described [25].

2.2 Chemical reagents

PF573228 (Sigma, 1 μ M) and PP2 (Sigma, 10 μ M) were used to inhibit FAK and Src, respectively. Compound C (Millipore Sigma, 5 μ M) and A769662 (Tocris, 25 μ M) were used as a global AMPK inhibitor and activator, respectively.

2.3 Cell culture and transfection

The human breast cancer cell line MDA-MB-231 and human mammary epithelial cell line MCF-10A were used. MDA-MB-231 cells were cultured in Dulbecco's modified Eagle's medium (DMEM, Lonza) supplemented with 10% FBS (Gibco) and 1% penicillin/streptomycin (Lonza). MCF-10A cells were cultured in DMEM/F12 (Gibco) supplemented with 10% FBS (Gibco), 1% penicillin/streptomycin (Lonza), 200 ng/mL human recombinant EGF, 50 μ g/mL hydrocortisone, and 20 μ g/mL insulin (Sigma). All cells were maintained at 37 °C and 5% CO₂ in a humidified incubator. For transfection, lipofectamine LTX (Invitrogen) was used following the manufacturer's protocol. Prior to experimentation, transfected cells were transferred to type I collagen-coated glass-bottom dishes (MatTek) or μ -slide cell culture chambers (Ibidi) and incubated for at least 2 hours.

2.4 Collagen-Matrigel preparation and characterization

For 3D experiments, cells were seeded in type I collagen-Matrigel consisting of 1 part antibiotic-free DMEM (10X), 8 parts PureCol type I collagen solution (Advanced BioMatrix, 3 mg/mL), and 1 part Matrigel (Corning, 9.8 mg/mL). The pH of the mixture was adjusted to 7.4 using sterile NaOH or HCl. The complete collagen-Matrigel solution was warmed to room temperature, and cells were suspended in the mixture at a density of 1×10^6 cells/mL. For 3D experiments, 100 μ L of the mixture was added into a glass-bottom dish (MatTek) or injected into a μ -slide cell culture chamber (Ibidi). Cell-gel mixtures were incubated for 2 hours at 37 °C and 5% CO₂ to form gel. Once gelation was complete, low-serum (1% FBS), antibiotic-free DMEM was added to each dish or chamber, and the samples were incubated for at least 2 hours before imaging. The interstitial flow speed through the 3D collagen-Matrigel was calculated by measuring the intensity of fluorescent probes moving through the cell-gel construct over time [26]. Briefly, fluorescent images were taken of collagen gel inside the flow chamber before the addition of fluorescent probes, providing a reference for background intensity. Next, Alexa Fluor 594-conjugated bovine serum albumin (BSA-594, Thermo Fisher, 50 μ g/ml) was added to the FluoroBrite DMEM (Gibco) that perfused the flow chamber. Using the syringe pump, the fluorescent media was delivered through the gel construct at known volumetric flow rates (2, 5, 10 μ L/min). Fluorescent images were obtained every minute for 10 minutes to track the perfusion of BSA-594 through the collagen gel. This range of interstitial flow speed yields a corresponding range of fluid shear stress exerted on cells embedded in the collagen-Matrigel which was found to be 2-10 dyne/cm² [26].

2.5 Shear stress application

Fluid flow-induced shear stress was applied to both 2D and 3D cell samples grown in μ -slide cell culture chambers (Ibidi). For 2D samples, unidirectional flow was applied with phenol red-free DMEM (HyClone) supplemented with 1% FBS using a peristaltic pump (Cole-Parmer). The shear stress of 10 dyne/cm² was applied by controlling the flow rate of the pump. The necessary flow rate was calculated according to the manufacture's protocol. For 3D collagen gel samples, a unidirectional, pulsatile (0.2 Hz) flow was applied using a syringe pump (Harvard Apparatus) [26]. Three different flow rates (2, 5, 10 μ L/min) were used to generate a range of shear stresses on the cells [26]. The flow chamber was connected to the syringe pump via sterile tubing filled with FluoroBrite DMEM (Gibco) with 1% FBS. Shear stress experiments were conducted at 37 °C and 5% CO₂ using a humidified incubation chamber (Ibidi).

2.6 Random migration assay

Cells were first incubated for 30 minutes with CellTracker Green CMFDA (Thermo Fisher, 20 μ M). Cells were then seeded at low (10-20%) confluency on μ -slide flow chambers (Ibidi) coated with type I collagen (Advanced Biomatrix, 100 μ g/mL), and incubated for 2 hours. Flow chambers were then subjected to 0 or 10 dyne/cm² for 8 hours. For some experiments, cells were treated with Compound C or A769662, or transfected with mito-AIP. Antibiotic-free, phenol red-free DMEM (1% FBS) was used for all migration experiments. Flow chambers were kept at 37 °C and 5% CO₂ inside a humidified incubation chamber (Ibidi) during the migration assay. Imaging regions were selected to include multiple isolated cells, away from the chamber walls and free to migrate randomly [27].

2.7 Microscopy and image analysis

All images were captured using a Nikon Ti-E inverted microscope equipped with an Evolve 512 EMCCD camera (Photometrics) and Perfect Focus System (Nikon). FRET images were acquired using CFP 438 excitation, CFP 483 emission, and YFP 542 emission wavelength filters. Green fluorescent images were captured using a GFP 522 emission wavelength filter. To reduce photobleaching, a neutral density (ND) 32 filter was used with the HG lamp (Nikon). For IFF experiments, FRET and DIC images were taken every 2 minutes for 1 hour using a 40× objective. FRET ratio images for Src, FAK, and AMPK biosensors were created using NIS-Elements software (Nikon) and ImageJ [26]. For cell migration experiments, images of DIC and GFP were taken every 5 minutes for 8 hours using a 15× objective. Cell tracking was conducted using the ImageJ plugin TrackMate [28]. Isolated cells that stayed within the image frame, did not divide, and did not die during the 8 hours were selected. Average distance traveled was calculated in Excel (Microsoft).

2.8 Statistical analysis

Three independent experiments were conducted for each condition. All statistical data are shown as the mean \pm standard error of the mean (SEM). Statistical significance between multiple groups was determined using one-way analysis of variance (ANOVA) with Dunnett's post hoc test. Statistical significance between two groups was assessed using Student's t-test. All statistical analysis was completed using Prism 5 software (GraphPad). A p-value less than 0.05 was considered statistically significant.

3. Results

3.1 IFF induces Mito-AMPK activity in MDA-MB-231 cells

Since we hypothesized that subcellular compartment-specific AMPK might have distinct roles in cancer progression under flow, we first tested whether AMPK differently responds to IFF depending on the subcellular locations. The results revealed that only Mito-AMPK was significantly upregulated in response to 5 and 10 $\mu\text{L}/\text{min}$ in MDA-MB-231 cells and the lowest flow rate (2 $\mu\text{L}/\text{min}$) did not significantly affect Mito-AMPK activity, suggesting the existence of the threshold for the flow-induced AMPK activity (Fig. 1A). Cyto-, PM-, and Nuc-AMPK were not activated by IFF in MDA-MB-231 cells. Next, we compared subcellular AMPK responses to IFF in cancer cells and normal cells. None of the biosensors displayed significant activation in MCF-10A cells (Fig. 1B). These data suggest that MDA-MB-231 cells and MCF-10A cells might have different mechanosensitivity, and that AMPK at the mitochondria might have a distinct role in MDA-MB-231 cells under IFF.

3.2 Inhibition of FAK or Src abolishes IFF-induced Mito-AMPK activity

To determine the role of FAK and Src in AMPK activity, we first investigated the mechanotransduction of FAK and Src in MDA-MB-231 cells. Application of 10 $\mu\text{L}/\text{min}$ IFF induced significant FAK activation, while 2 and 5 $\mu\text{L}/\text{min}$ did not alter FAK (Fig. 2A). Src was also significantly activated by IFF in MDA-MB-231 cells. The 5 and 10 $\mu\text{L}/\text{min}$ IFF activated Src with similar efficacy. Next, MDA-MB-231 cells transfected with Mito-AMPK were embedded in collagen-Matrigel and then incubated with either PF573228 or PP2. Both Src and FAK inhibition resulted in consistently lower Mito-AMPK activity compared to the untreated cells (Fig. 2B). Next, we sought to determine whether this inhibition could affect IFF-induced Mito-AMPK activity. The results revealed that inhibition of FAK or Src abolished IFF-induced

Mito-AMPK activity, suggesting that FAK and Src are required for the flow-mediated mechanotransduction of AMPK at the mitochondria (Fig. 2C).

3.3 Global AMPK activation reduces cancer cell migration

To determine whether AMPK affects migratory behavior of MDA-MB-231 cells, we conducted a random migration assay. Results showed a significant decrease in cell migration in response to global AMPK activation (Fig. 3A). The average cell displacement for untreated cells was $158.0 \pm 6.8 \mu\text{m}$, while the average displacement for cells treated with A769662 was $104.0 \pm 3.4 \mu\text{m}$ (a 34% decrease). However, cells treated with Compound C did not show a significant difference in cell migration compared to the control. These results are consistent with published reports on the linkage of global AMPK activation and the decreased migration or invasion of many cancers, including breast cancer [14, 18].

3.4 Mitochondria-specific AMPK inhibition reduces cancer cell migration

Since we observed that IFF increased AMPK activity at the mitochondria in MDA-MB-231 cells (Fig. 1), we sought to determine the role of mitochondria-specific AMPK in cancer cell migration. MDA-MB-231 cells transfected with mito-AIP showed significantly reduced cell migration although to a lesser degree compared to the A769662-treated cells (Fig. 3A). The average cell displacement for mito-AIP transfected cells was $136.0 \pm 5.3 \mu\text{m}$ (14% decrease) compared to the control group (Fig. 3B). To ensure that decreased migration was not simply a result of transfection, cells transfected with a transfection reagent alone as well as a Mito-AMPK biosensor were compared with the control group. Transfection did not significantly affect cell migration (data not shown).

3.5 Mitochondria-specific AMPK inhibition blocks flow-induced cell migration

To further investigate the role of AMPK activity at the mitochondria in cancer cell migration, we conducted a cell migration assay under flow conditions. MDA-MB-231 cells were plated in collagen-coated flow chambers and subjected to fluid flow at 10 dyne/cm². Cells subjected to 8 hours of fluid flow showed a significant increase in cell migration compared to the control group (Fig. 3A, B). This confirmed the notion that fluid shear stress increases cancer cell metastatic potential. Next, cells were transfected with mito-AIP and then subjected to 10 dyne/cm² fluid flow. Mitochondria-specific AMPK inhibition abolished the migration response to fluid flow (Fig. 3A). The average cell displacement was reduced to $132.1 \pm 6.9 \mu\text{m}$, a 16.4% decrease compared to the control group (Fig. 3B). To test whether suppressed cell migration by mito-AIP is due to the effect of decreased AMPK activity at the mitochondria, we measured subcellular AMPK activity with and without mito-AIP treatment. Transfection with mito-AIP significantly increased cytosolic AMPK while decreasing mitochondria AMPK (Fig. 3C). This result is in line with the notion that AMPK at the mitochondria is primarily involved in ATP homeostasis through a feedback mechanism [25]. Taken together, these results suggest that cytosolic AMPK and mitochondrial AMPK might have a distinct, antagonistic role in breast cancer cell migration under flow.

4. Discussion

In this study we employed a 3D collagen-Matrigel model in conjunction with live cell imaging to visualize the activity of subcellular AMPK in response to IFF. We first examined subcellular compartment-specific AMPK activity under IFF in MDA-MB-231 cells and MCF-10A cells.

Interestingly, AMPK at the mitochondria in MDA-MB-231 cells exhibited an immediate response to IFF, while none of the AMPK in MCF-10A cells was responsive to IFF. This is in line with the previous findings that cancer cells are sensitive to abnormal mechanical environments such as stiffer extracellular matrix stiffness and increased IFF [3, 22, 29]. The molecular mechanism of distinct AMPK response to IFF at the mitochondria is not clear, but one speculation would be that mitochondria is perturbed by extracellular mechanical stresses through the cytoskeleton [30]. A recent report also suggests that AMPK activation by mechanical stresses requires cytoskeleton-mediated intracellular contractility [31].

We identified AMPK at the mitochondria as a potential downstream target of FAK/Src signaling in response to IFF. FAK and Src play a primary role in integrin-dependent mechanotransduction in tumor tissues as well as many other tissues [32, 33]. We showed here that inhibition of FAK or Src suppressed the basal activation level of Mito-AMPK and blocked IFF-induced Mito-AMPK activation. To our knowledge, this is the first report that describes the involvement of FAK and Src in the mechanotransduction of mitochondria-specific AMPK. AMPK has been shown to mediate integrin $\beta 1$ [34] as well as FAK [35]. On the contrary, AMPK is mediated through Src [36, 37]. Together with these data, our results suggest that there might be a feedback loop in mechanotransduction between FAK/Src and AMPK.

Our data also highlight the importance of AMPK at the mitochondria in cell migration.

Mitochondria regulate calcium homeostasis needed for polarity and cell migration and MDA-MB-231 cells cannot migrate effectively when mitochondrial genes are perturbed [38]. During cell migration, mitochondria reposition strategically along microtubules, which polymerize

toward cellular extensions [38-40]. AMPK controls the speed of microtubule polymerization toward focal adhesions [40], and AMPK activation localizes at the mitochondria as they were trafficked toward the leading edge of cells during migration [39]. Several lines of evidence including our data in the present study indicate that global AMPK activation reduces cell migration [14, 18]. We observed here that inhibition of AMPK at the mitochondria increased the activation level of cytosolic AMPK in MDA-MB-231 cells, which might negatively affect cell migration. In conclusion, our results suggest that localized AMPK activities at various subcellular domains may have unique or even antagonistic functions, particularly in MDA-MB-231 cells.

Acknowledgements

We thank J. Zhang (University of California San Diego, USA) and T. Inoue (Johns Hopkins University, USA) for the gift of the AMPK biosensors, and Y. Wang (University of California San Diego, USA) for the gift of the FAK and Src biosensors. This work was supported in part by the 100 Voices of Hope; and the Biomechanics and Biomaterials Research Center – Integrated Nanosystems Development Institute at the IUPUI.

References

- [1] R.K. Jain, J.D. Martin, T. Stylianopoulos, The role of mechanical forces in tumor growth and therapy, *Annu Rev Biomed Eng*, 16 (2014) 321-346.
- [2] C.H. Heldin, K. Rubin, K. Pietras, A. Ostman, High interstitial fluid pressure - an obstacle in cancer therapy, *Nat Rev Cancer*, 4 (2004) 806-813.

- [3] J.M. Munson, A.C. Shieh, Interstitial fluid flow in cancer: implications for disease progression and treatment, *Cancer Manag Res*, 6 (2014) 317-328.
- [4] A.C. Shieh, Biomechanical forces shape the tumor microenvironment, *Ann Biomed Eng*, 39 (2011) 1379-1389.
- [5] M.J. Mitchell, M.R. King, Computational and experimental models of cancer cell response to fluid shear stress, *Front Oncol*, 3 (2013) 44.
- [6] W.J. Polacheck, J.L. Charest, R.D. Kamm, Interstitial flow influences direction of tumor cell migration through competing mechanisms, *Proc Natl Acad Sci U S A*, 108 (2011) 11115-11120.
- [7] L. Chin, Y. Xia, D.E. Discher, P.A. Janmey, Mechanotransduction in cancer, *Curr Opin Chem Eng*, 11 (2016) 77-84.
- [8] W.J. Polacheck, A.E. German, A. Mammoto, D.E. Ingber, R.D. Kamm, Mechanotransduction of fluid stresses governs 3D cell migration, *Proc Natl Acad Sci U S A*, 111 (2014) 2447-2452.
- [9] T. Oskarsson, Extracellular matrix components in breast cancer progression and metastasis, *Breast*, 22 Suppl 2 (2013) S66-72.
- [10] Y.L. Tai, L.C. Chen, T.L. Shen, Emerging roles of focal adhesion kinase in cancer, *Biomed Res Int*, 2015 (2015) 690690.
- [11] S.K. Mitra, D.D. Schlaepfer, Integrin-regulated FAK-Src signaling in normal and cancer cells, *Curr Opin Cell Biol*, 18 (2006) 516-523.
- [12] C.M. Bagi, G.W. Roberts, C.J. Andresen, Dual focal adhesion kinase/Pyk2 inhibitor has positive effects on bone tumors: implications for bone metastases, *Cancer*, 112 (2008) 2313-2321.
- [13] R.S. Finn, Targeting Src in breast cancer, *Ann Oncol*, 19 (2008) 1379-1386.

- [14] W. Li, S.M. Saud, M.R. Young, G. Chen, B. Hua, Targeting AMPK for cancer prevention and treatment, *Oncotarget*, 6 (2015) 7365-7378.
- [15] A.S. Khan, D.E. Frigo, A spatiotemporal hypothesis for the regulation, role, and targeting of AMPK in prostate cancer, *Nat Rev Urol*, 14 (2017) 164-180.
- [16] G. Zadra, J.L. Batista, M. Loda, Dissecting the Dual Role of AMPK in Cancer: From Experimental to Human Studies, *Mol Cancer Res*, 13 (2015) 1059-1072.
- [17] B. Faubert, E.E. Vincent, M.C. Poffenberger, R.G. Jones, The AMP-activated protein kinase (AMPK) and cancer: many faces of a metabolic regulator, *Cancer Lett*, 356 (2015) 165-170.
- [18] Y. Yan, O. Tsukamoto, A. Nakano, H. Kato, H. Kioka, N. Ito, S. Higo, S. Yamazaki, Y. Shintani, K. Matsuoka, Y. Liao, H. Asanuma, M. Asakura, K. Takafuji, T. Minamino, Y. Asano, M. Kitakaze, S. Takashima, Augmented AMPK activity inhibits cell migration by phosphorylating the novel substrate Pdlim5, *Nat Commun*, 6 (2015) 6137.
- [19] M. Kodiha, J.G. Rassi, C.M. Brown, U. Stochaj, Localization of AMP kinase is regulated by stress, cell density, and signaling through the MEK-->ERK1/2 pathway, *Am J Physiol Cell Physiol*, 293 (2007) C1427-1436.
- [20] J. Creighton, Targeting therapeutic effects: subcellular location matters. Focus on "Pharmacological AMP-kinase activators have compartment-specific effects on cell physiology", *Am J Physiol Cell Physiol*, 301 (2011) C1293-1295.
- [21] M. Kodiha, A. Salimi, Y.M. Wang, U. Stochaj, Pharmacological AMP kinase activators target the nucleolar organization and control cell proliferation, *PLoS One*, 9 (2014) e88087.
- [22] J.C. Tung, J.M. Barnes, S.R. Desai, C. Sistrunk, M.W. Conklin, P. Schedin, K.W. Eliceiri, P.J. Keely, V.L. Seewaldt, V.M. Weaver, Tumor mechanics and metabolic dysfunction, *Free Radic Biol Med*, 79 (2015) 269-280.

- [23] Y. Wang, E.L. Botvinick, Y. Zhao, M.W. Berns, S. Usami, R.Y. Tsien, S. Chien, Visualizing the mechanical activation of Src, *Nature*, 434 (2005) 1040-1045.
- [24] J. Seong, M. Ouyang, T. Kim, J. Sun, P.C. Wen, S. Lu, Y. Zhuo, N.M. Llewellyn, D.D. Schlaepfer, J.L. Guan, S. Chien, Y. Wang, Detection of focal adhesion kinase activation at membrane microdomains by fluorescence resonance energy transfer, *Nat Commun*, 2 (2011) 406.
- [25] T. Miyamoto, E. Rho, V. Sample, H. Akano, M. Magari, T. Ueno, K. Gorshkov, M. Chen, H. Tokumitsu, J. Zhang, T. Inoue, Compartmentalized AMPK signaling illuminated by genetically encoded molecular sensors and actuators, *Cell Rep*, 11 (2015) 657-670.
- [26] Q. Wan, T. TruongVo, H.E. Steele, A. Ozcelikkale, B. Han, Y. Wang, J. Oh, H. Yokota, S. Na, Subcellular domain-dependent molecular hierarchy of SFK and FAK in mechanotransduction and cytokine signaling, *Sci Rep*, 7 (2017) 9033.
- [27] B.D. Riehl, J.S. Lee, L. Ha, J.Y. Lim, Fluid-flow-induced mesenchymal stem cell migration: role of focal adhesion kinase and RhoA kinase sensors, *J R Soc Interface*, 12 (2015).
- [28] J.Y. Tinevez, N. Perry, J. Schindelin, G.M. Hoopes, G.D. Reynolds, E. Laplantine, S.Y. Bednarek, S.L. Shorte, K.W. Eliceiri, TrackMate: An open and extensible platform for single-particle tracking, *Methods*, 115 (2017) 80-90.
- [29] F. Broders-Bondon, T.H. Nguyen Ho-Boulidoires, M.E. Fernandez-Sanchez, E. Farge, Mechanotransduction in tumor progression: The dark side of the force, *J Cell Biol*, 217 (2018) 1571-1587.
- [30] N. Wang, J.D. Tytell, D.E. Ingber, Mechanotransduction at a distance: mechanically coupling the extracellular matrix with the nucleus, *Nat Rev Mol Cell Biol*, 10 (2009) 75-82.

- [31] J.L. Bays, H.K. Campbell, C. Heidema, M. Sebbagh, K.A. DeMali, Linking E-cadherin mechanotransduction to cell metabolism through force-mediated activation of AMPK, *Nat Cell Biol*, 19 (2017) 724-731.
- [32] A.D. Bershadsky, N.Q. Balaban, B. Geiger, Adhesion-dependent cell mechanosensitivity, *Annu Rev Cell Dev Biol*, 19 (2003) 677-695.
- [33] M.A. Schwartz, Integrins and extracellular matrix in mechanotransduction, *Cold Spring Harb Perspect Biol*, 2 (2010) a005066.
- [34] M. Georgiadou, J. Lilja, G. Jacquemet, C. Guzman, M. Rafeeva, C. Alibert, Y. Yan, P. Sahgal, M. Lerche, J.B. Manneville, T.P. Makela, J. Ivaska, AMPK negatively regulates tensin-dependent integrin activity, *J Cell Biol*, 216 (2017) 1107-1121.
- [35] D.G. Lassiter, C. Nylen, R.J.O. Sjogren, A.V. Chibalin, H. Wallberg-Henriksson, E. Naslund, A. Krook, J.R. Zierath, FAK tyrosine phosphorylation is regulated by AMPK and controls metabolism in human skeletal muscle, *Diabetologia*, 61 (2018) 424-432.
- [36] M.H. Zou, X.Y. Hou, C.M. Shi, S. Kirkpatrick, F. Liu, M.H. Goldman, R.A. Cohen, Activation of 5'-AMP-activated kinase is mediated through c-Src and phosphoinositide 3-kinase activity during hypoxia-reoxygenation of bovine aortic endothelial cells. Role of peroxynitrite, *J Biol Chem*, 278 (2003) 34003-34010.
- [37] S. Mizrachi-Schwartz, N. Cohen, S. Klein, N. Kravchenko-Balasha, A. Levitzki, Up-regulation of AMP-activated protein kinase in cancer cell lines is mediated through c-Src activation, *J Biol Chem*, 286 (2011) 15268-15277.
- [38] V. Paupe, J. Prudent, New insights into the role of mitochondrial calcium homeostasis in cell migration, *Biochem Biophys Res Commun*, 500 (2018) 75-86.

[39] B. Cunniff, A.J. McKenzie, N.H. Heintz, A.K. Howe, AMPK activity regulates trafficking of mitochondria to the leading edge during cell migration and matrix invasion, *Mol Biol Cell*, 27 (2016) 2662-2674.

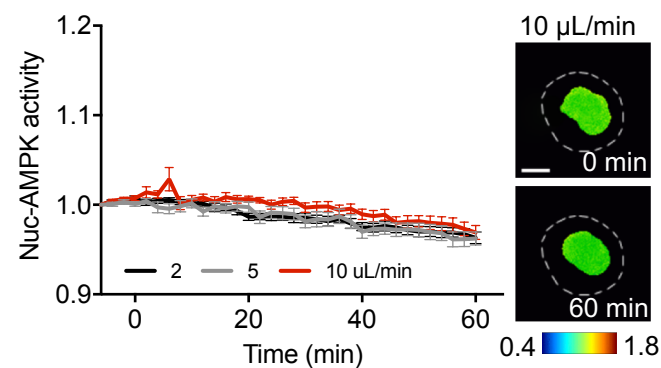
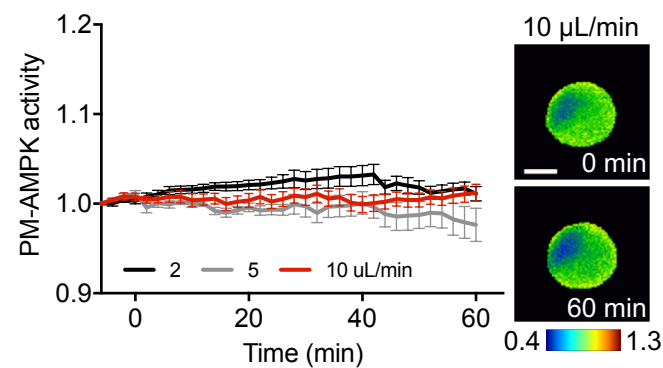
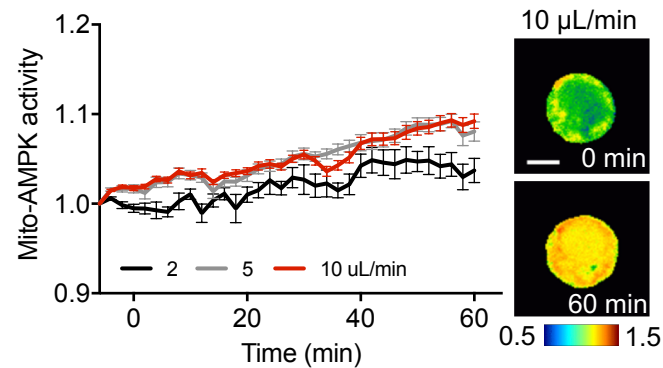
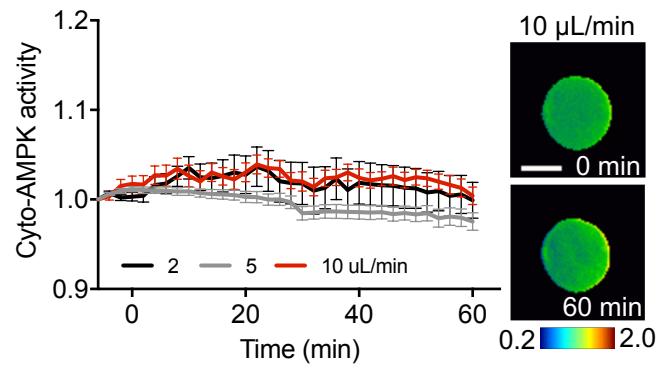
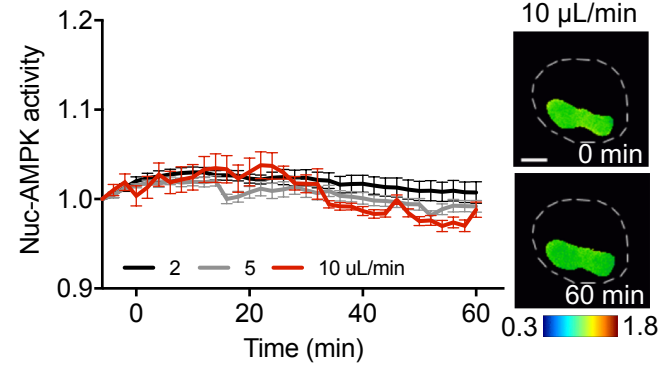
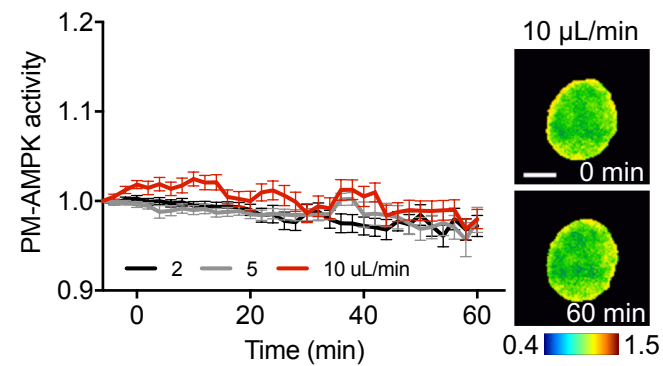
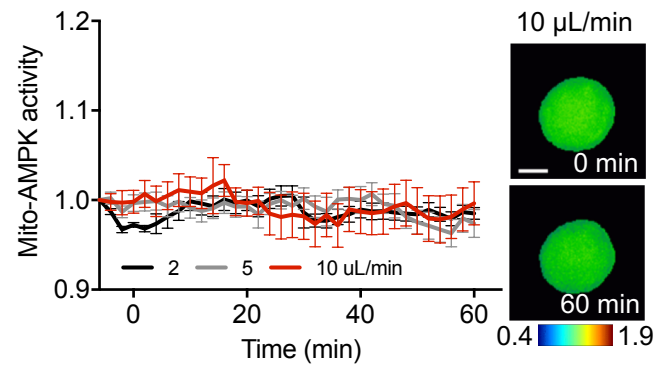
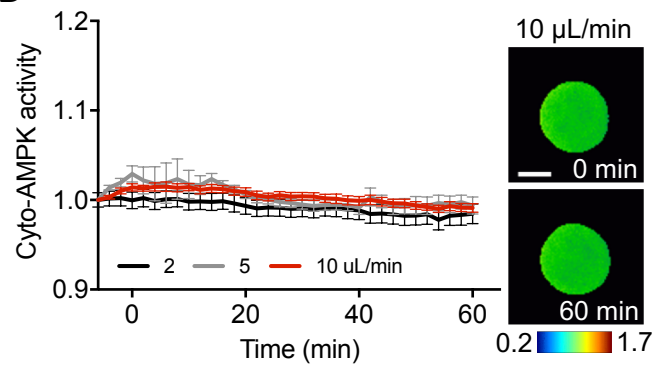
[40] A. Nakano, H. Kato, T. Watanabe, K.D. Min, S. Yamazaki, Y. Asano, O. Seguchi, S. Higo, Y. Shintani, H. Asanuma, M. Asakura, T. Minamino, K. Kaibuchi, N. Mochizuki, M. Kitakaze, S. Takashima, AMPK controls the speed of microtubule polymerization and directional cell migration through CLIP-170 phosphorylation, *Nat Cell Biol*, 12 (2010) 583-590.

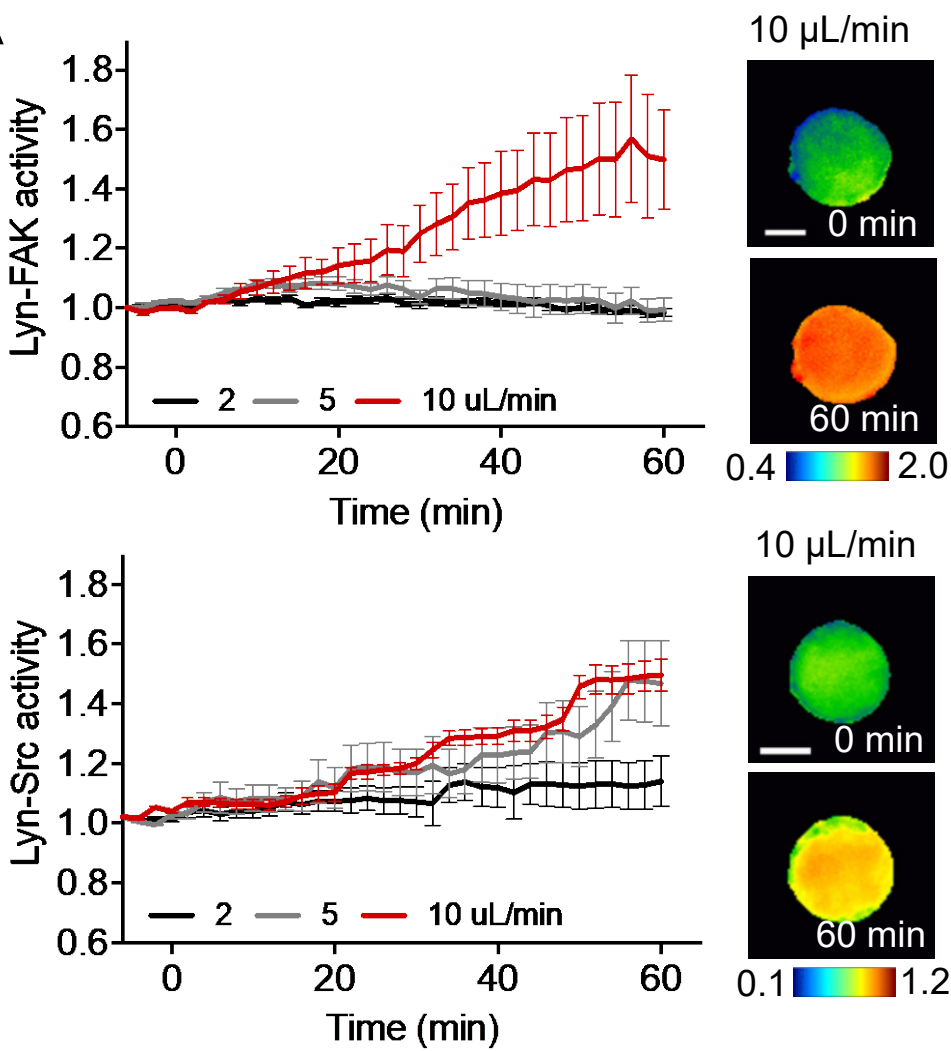
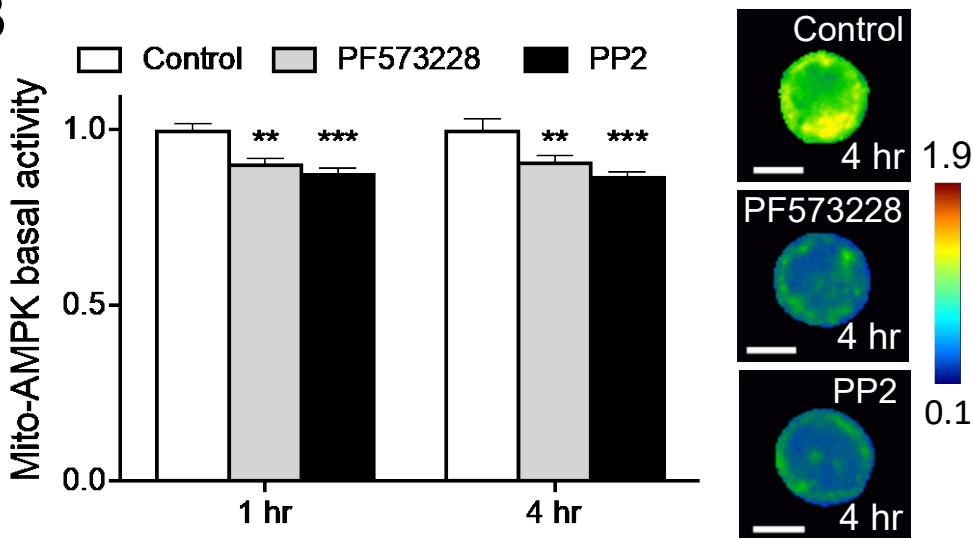
Figure legends

Figure 1. AMPK activities at subcellular compartments in response to IFF. FRET ratio images were scaled according to the color bar. IFF was applied at time = 0 min. (A) MDA-MB-231 cells. Cyto-AMPK: n=13, 16, 11 (2, 5, 10 μ L/min, respectively); Mito-AMPK: n=12, 14, 13 (2, 5, 10 μ L/min, respectively); PM-AMPK: n=11, 11, 12 (2, 5, 10 μ L/min, respectively); Nuc-AMPK: n=14, 12, 16 (2, 5, 10 μ L/min, respectively). (B) MCF-10A cells. Cyto-AMPK: n=12, 10, 20 (2, 5, 10 μ L/min, respectively); Mito-AMPK: n=13, 13, 13 (2, 5, 10 μ L/min, respectively); PM-AMPK: n=14, 14, 14 (2, 5, 10 μ L/min, respectively); Nuc-AMPK: n=16, 14, 14 (2, 5, 10 μ L/min, respectively). Scale bars, 10 μ m. * p<0.05.

Figure 2. Involvement of FAK and Src in Mito-AMPK activity. Scale bars, 10 μ m. (A) FAK and Src activity in MDA-MB-231 cells under IFF. FAK: n=10, 8, 8 (2, 5, 10 μ L/min, respectively). Src: n=9, 9, 8 (2, 5, 10 μ L/min, respectively). (B) Mito-AMPK basal activity in MDA-MB-231 cells after treatment with PF573228 or PP2. n>13. ** p<0.01, *** p<0.001. (C) Mito-AMPK response to IFF in MDA-MB-231 cells pre-treated with PF573228 or PP2. n>14.

Figure 3. Cell migration is uniquely influenced by subcellular AMPK. (A) Cell trajectories. For visual comparison, the trajectories of 25 randomly selected cells are shown. (B) Average displacement of cells over 8 hours. Control, n=30; A769962, n=54; Compound C, n=64; mito-AIP, n=36; fluid flow, n=41; fluid flow + mito-AIP, n=39. (C) Subcellular compartment-specific AMPK activities in response to mito-AIP. n>20. * p<0.05. *** p<0.001.

A**B**

A**B****C**